Joint Pathology Center

Veterinary Pathology Services

WEDNESDAY SLIDE CONFERENCE 2016-2017

C o n f e r e n c e 21

31 March 2017

Linden Craig, DVM, PhD, Diplomate ACVP
Professor of Anatomic Pathology
University of Tennessee College of Veterinary Medicine

CASE I: 12B2212 (JPC 4050655).

Signalment: Nine-year-old castrated male Labrador retriever (*Canis familiaris*).

History: Right pelvic limb swelling noticed in July 2012. Treated with prednisone, diphenhydramine, cephalexin. Viscous fluid aspirate from limb 8/8/12. Presented to Internal Medicine 9/4/12 - chest x-rays unremarkable, right pelvic limb x-rays showed an aggressive lesion involving distal femur, with soft tissue swelling involving down to distal tibia. Aspiration cytology - probable sarcoma.

Abdominal ultrasound and pelvic CT scan showed a large cystic mass involving the right pelvic limb with bone invasion and presumed metastasis to the right inguinal and right medial iliac lymph node. Possible femoral vein thrombus. High coxofemoral disarticulation amputation performed. Clinical diagnosis: Sarcoma with lymph node metastasis.

Gross Pathology: A right pelvic limb from the femoral head and distally was submitted. The stifle joint and muscles of the thigh were expanded by palpably viscous, coalescing nodules. The popliteal lymph node was bi-lobed and measured approximately 2.6 x 1.4 x 1 cm. On cut surface, was mottled dull yellow, red to red-brown, slightly bulging and contained multifocal to coalescing round to oval, 0.2-0.5cm, soft to firm cystic structures filled alternatively with small amounts of clear, colorless fluid to opaque, firm, off-white material. On cut surface, the stifle joint was expanded by a 5x6x5cm, mottled dull yellow, red to red-brown, slightly bulging mass of multifocal to coalescing round to oval, soft to firm cyst-like structures that were filled alternatively with small amounts of clear, colorless fluid to opaque, firm, off-white material. Large amounts of mucoid, gelatinous, dull, yellow-red material expanded fascial planes, lymphatic vessels, and subcutaneous tissues from the mid-femur distally, and most severely, along the proximal and mid-tibia. The stifle joint was

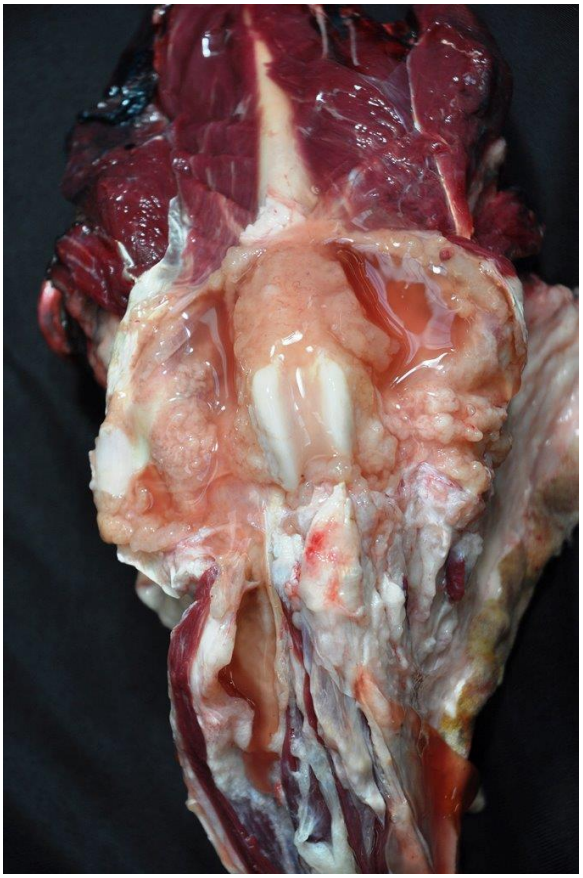

Stifle, dog. The joint is expanded by a 5x6x5cm, by a slightly bulging mass of composed of cyst-like structures that contain clear to slightly opaque material. (Photo courtesy of: University of California, Davis School of Veterinary Medicine, Veterinary Medical Teaching Hospital, Anatomic Pathology Department http://www.vetmed.ucdavis.edu/vmth/small_animal/anatomic_pathology/)

expanded by approximately 40 ml of the same material. The synovium of the stifle joint was diffusely thickened with papillary and ovoid projections and cavitations as previously described in the popliteal lymph node. The joint capsule as variably friable to firm. The entire limb was sagittally sectioned and on cut surface a firm to soft mass composed of thousands of small, firm, semi-transparent, off-white nodules emanated from the plantar aspect of the level of the stifle joint. The mass compressed the normal structures of the region. Approximately 3-5 small (0.8x0.5cm), ovoid, firm, semi-translucent, off-white masses tracked along and were adhered the femoral vasculature adventitia, including approximately 1.0cm from the surgical margin.

The inguinal lymph node was also submitted and measured 6 x 3.5 x 1.8 cm and on cut surface is expanded by multilobulated, multicavitated nodules that vary in size from 0.9 cm to 1.3 cm in diameter. They are round to oval and contain variable amounts of mucoid, tenacious, clear, colorless fluid.

Laboratory results: Radiographic findings: There is marked soft tissue swelling surrounding the tibia and loss of the normal fascial plane distinction. There are lobular soft tissue densities at the medial aspect of the right stifle joint. There is permeative lysis of the distal femur, resulting in a coarse trabecular pattern and sclerosis with an indistinct transition zone between normal and abnormal bone. Periarticular osteophytes are present on the apex of the patella, the fabellae, the proximal tibia, and the distal femur. There is marked increased soft tissue opacity associated with the stifle joint.

Stifle, dog. Sagittal section of the stifle joint showing extension of the neoplasm into adjacent skeletal muscle into adjacent muscle and subcutis. (Photo courtesy of: University of California, Davis School of Veterinary Medicine, Veterinary Medical Teaching Hospital, Anatomic Pathology Department http://www.vetmed.ucdavis.edu/vmth/small_animal/anatomic_pathology/)

Radiographic Impressions: Aggressive bone lesion affecting the distal right femur with adjacent lobular soft tissue opacities is concerning for a soft tissue neoplasm with extension to the bone such as a synovial cell sarcoma. Mild secondary joint disease. Marked edema of the right crus. An ultrasound examination of the right stifle is recommended if clinically indicated. Pulmonary osteomas. No radiographic evidence of pulmonary metastatic disease.

CT Scanning impressions: Large cystic right pelvic limb mass with associated sub-cutaneous edema and bone invasion. Filling defect of the right femoral vein may be secondary to tumor invasion or thrombus formation. Metastatic inguinal and sub-lumbar lymph nodes. The appearance of the right hypogastric and mesenteric lymph nodes may represent metastases or reactivity.

Cytology of stifle mass: Four moderately cellular coverslips are examined that have a medium pink stippled background and a mild amount of blood with erythrocytes frequently distributed in a prominent windrowing pattern. Nucleated cells are distributed individually and in variably sized loose aggregates. Thick pink fibrillar material is frequently seen associated with cell aggregates. Individual cells consist predominantly of macrophages / synoviocytes. Cells in clusters have a low to moderate amount of pale cytoplasm that frequently causes polar wisps giving the cells a spindloid shape. Nuclei are ovoid with coarsely stippled chromatin and small nucleoli. Low numbers of small mature lymphocytes are also noted.

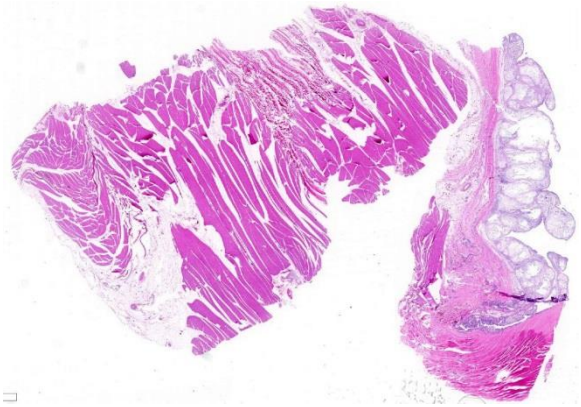

Stifle dog. Subgross view of submitted section with skeletal muscle at left, and mass arising to joint capsule at right. (HE, 4X)

Cytologic interpretation and comments: Probably sarcoma. The large aggregates of spindloid shape cells are consistent with a sarcoma, with considerations including spindle cell sarcoma, synovial sarcoma or even atypical chondrosarcoma, however, this is considered less likely.

Histopathologic Description: Examined are two cross sections of joint capsule which are markedly thickened up to 0.9 cm by a poorly cellular, abundantly myxoid, multinodular, unencapsulated, expansile neoplastic mass that primarily occupies the subintimal space. Individual variably-sized nodules are separated by thin bands of fibrous connective tissue. The neoplastic nodules often merge and are comprised of abundant amounts of lacy, gelatinous, pale, amphophilic to basophilic matrix and widely spaced stellate to spindloid cells. The cells are cytologically bland, have ill-defined borders and small amounts of a finely granular, eosinophilic cytoplasm. Nuclei are oval, with granular chromatin and variable numbers of ill-defined nucleoli. Aniso-cytosis and anisokaryosis are mild. No mitotic figures are observed. Multifocally along the most superficial aspects of the subintima, deep to synoviocytes, there are moderate to large numbers of lymphocytes and fewer plasma cells. Rarely, pigment-laden cells (macrophages) admix with the lymphocytes and plasma cells. The intimal

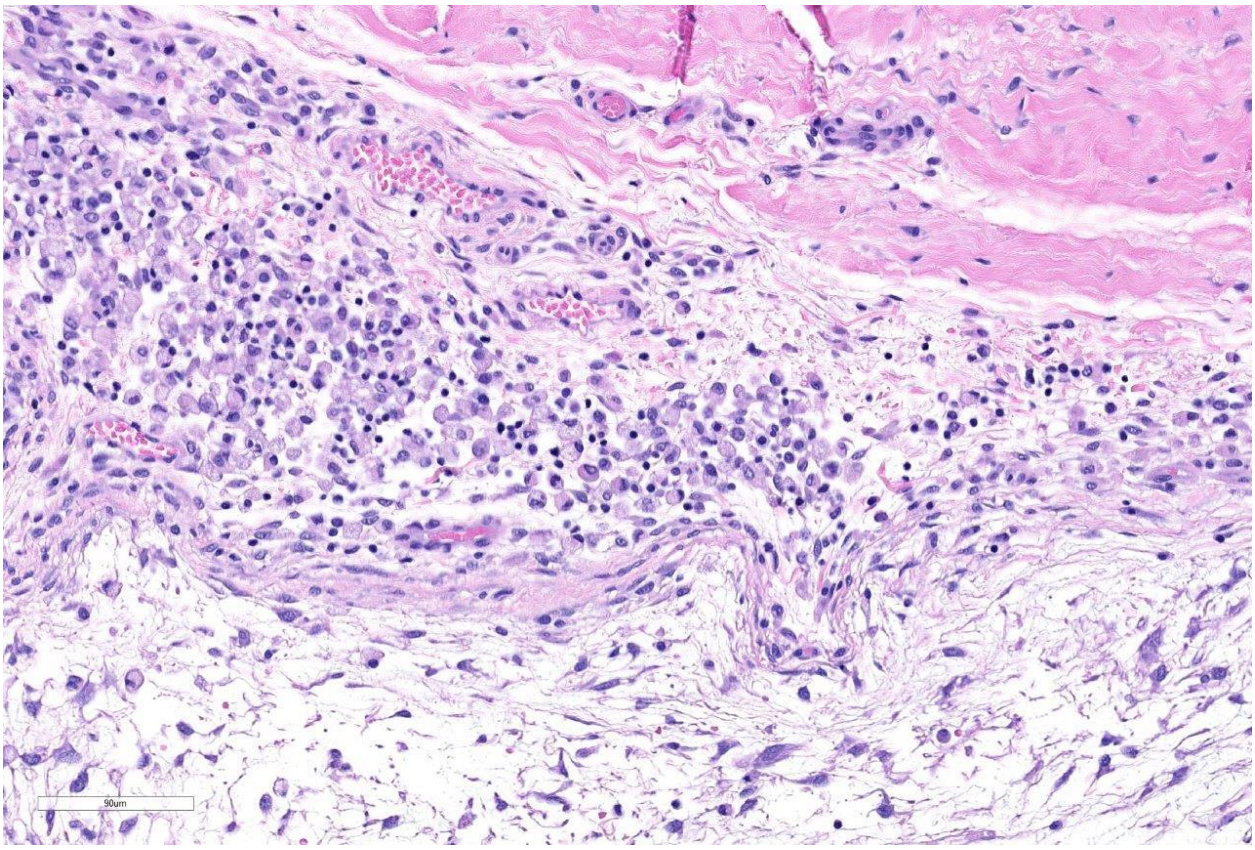

Stifle, dog. Higher magnification of the synovial neoplasm, demonstrated the multilobular nature, and myxomatous, occasionally cystic nature of the neoplasm. (HE, 16X)

layer is multifocally hyperplastic and jumbled up to 10 layers. The fibrous capsule is expanded by abundant fibrovascular tissue, adipose, and multifocal aggregates of plasma cells, lymphocytes, and fewer mast cells.

Contributor's Morphologic Diagnosis: Femorotibial (Stifle) Joint and associated skeletal muscle, Right Popliteal and Inguinal Lymph Nodes: Synovial myxoma with local invasion and multiple lymph node metastases

Contributor's Comment: Histiocytic sarcoma, synovial sarcoma, and synovial myxoma are three differentials for canine primary joint tumors.[2,3] All can cross joints and cause bony lysis and proliferation. Synovial myxoma occurs uncommonly in dogs and is widely considered to be a benign, but infiltrative, tumor of the joint. Numerous cases of lymph node metastases, however, have been observed (Contributing Institution experience). The stifle and digital joints are most commonly affected. The three types of cells in synovial membranes are Type A synoviocytes (macrophage/dendritic cell origin), type B (fibroblast-like), and type C ("transitional", hematopoietic, or stem cell-like). Although a joint tumor, the cell of origin of synovial myxomas is unknown; this is reflected in the non-specific immunohistochemistry (IHC). They are vimentin positive. Approximately 20-40% of synovial myxoma cells are CD18 immunoreactive and are morphologically indistinguishable from CD18 negative joint cells. Synovial myxomas are cadherin 11 and HSP25 immunoreactive, much like

synovial cell sarcomas and histiocytic sarcomas.[3] The most striking histologic feature of synovial myxomas is the sparse, stellate to spindle cells that elaborate abundant, coalescing nodules of myxomatous matrix.[2,3,5] Again, although cytomorphologic features are generally bland, synovial myxomas can metastasize to lymph nodes and be highly locally invasive.[2,3,5]

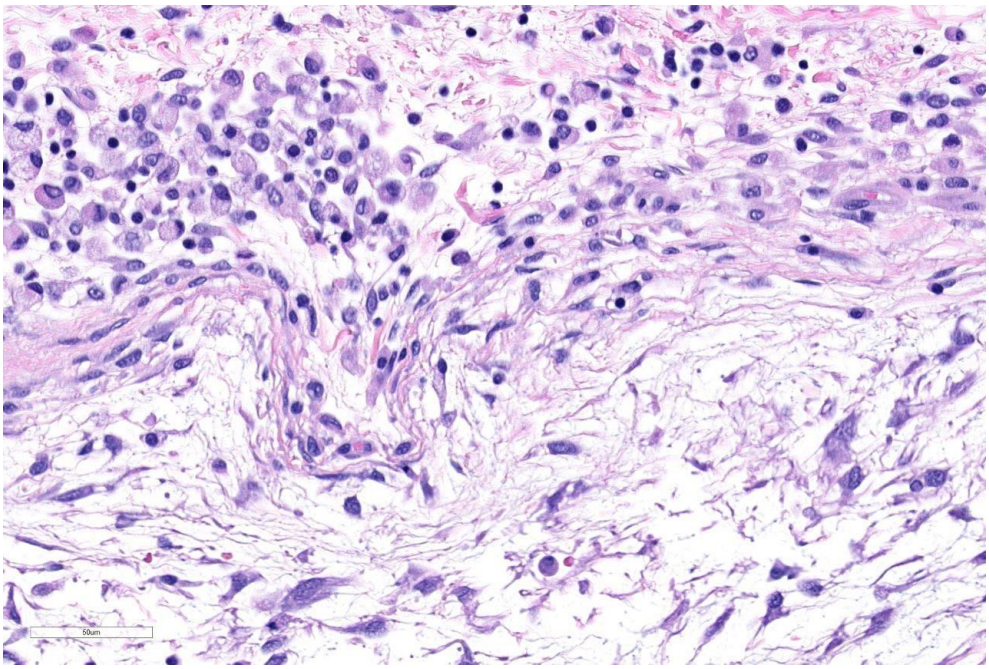

Stifle, dog. Neoplastic cells (at bottom) are spindled to stellate and separated by abundant myxomatous stroma. The periphery of the neoplasm contains numerous muciphages. (HE, 224X)

JPC Diagnosis: Joint, stifle (per contributor): Synovial myxoma, Labrador retriever, *Canis familiaris*.

Conference Comment: We thank the contributor for their institution's extensive work-up on this case and excellent quality gross images. Of the three differentials for canine joint neoplasms mentioned above, synovial myxoma is the second most common neoplasm occurring within the joints of dogs, behind histiocytic sarcoma and ahead of the rare synovial sarcoma (if such a tumor truly exists.) [1,3,4] This neoplasm most commonly affects middle-aged large breed dogs. Doberman pinschers and Labrador retrievers, as in this case, are most often affected. It has also been rarely reported in cats.[1,4] Synovial myxomas usually affect a single joint, with the stifle and digit the most commonly reported locations. These neoplasms are slow-growing and can persist for months to years and often present as chronic lameness with or without evidence of joint swelling.[1,3,4]

Although this is classified as a benign neoplasm, it can be locally infiltrative and cause lytic lesions in the bone with significant articular lesions and periarticular osteophyte formation. The conference moderator instructed that radiographically, synovial myxoma cannot be reliably differentiated from histiocytic sarcoma or synovial sarcoma.[3,4] Despite this locally invasive behavior, the prognosis is typically good after complete surgical excision. Bony lysis and infiltration usually necessitate amputation; however, cases that lack bone lysis and extension outside of the joint capsule can be treated with a simple synovectomy, which is curative in about 90% of reported cases. In contrast, histiocytic sarcomas are associated with a poor prognosis, with an average survival of just 5.3 months.[1,3,4] This significant

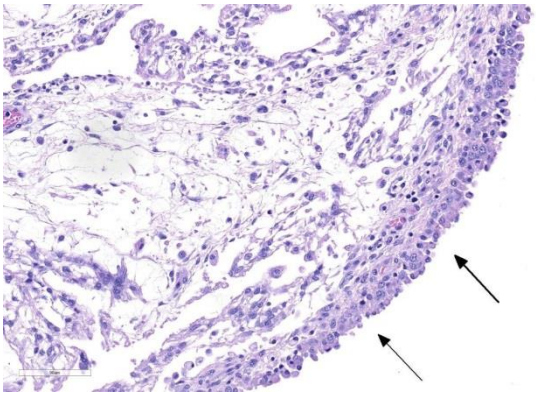

Stifle, dog. The surface of the neoplasm is covered by a layer of hyperplastic synovium up to 3 cell layers thick. (HE, 320X)

difference in biological behavior and prognosis highlights the importance of histopathology of the mass prior to treatment. Interestingly, the conference moderator and highly regarded veterinary pathologist with expertise in bone and joint pathology, Dr. Linden Craig, remarked that this is the first example of a synovial myxoma she has seen with metastasis. Given the observation by the contributor's intuition of multiple cases of lymph node metastasis for this neoplasm, Dr. Craig remarked that the biological behavior of this neoplasm may need further review.

Conference participants noted that once the tissue is identified as joint capsule with adjacent skeletal muscle, the diagnosis of synovial myxoma is relatively straight-forward. This neoplasm has a highly characteristic appearance of variably sized nodules of stellate to spindle cells with long cytoplasmic processes supported in a highly myxoid matrix and covered by a hyperplastic synovial lining.[1,3,4] The conference moderator noted that the cell of origin of synovial myxoma is not yet known; although, it is thought that given the abundant myxoid matrix, the cell type is likely type B (fibroblastic) synoviocytes. Type B synoviocytes normally produce hya-luronan, a large linear glycosaminoglycan and major component of synovial fluid.[1,3,4] Despite this uncertainty of cell origin, the diagnosis can usually be made without the aid of immuno-histochemical staining.

Contributing Institution:
University of California, Davis
School of Veterinary Medicine
Veterinary Medical Teaching Hospital
Anatomic Pathology Department
http://www.vetmed.ucdavis.edu/vmth/small_animal/anatomic_pathology/

References:

1. Craig LE, Ditmer KE, Thompson KG. Bones and joints. In Maxie, MG, ed. *Jubb, Kennedy, and Palmer's Pathology of Domestic Animals*, Vol I. 6th ed. Philadelphia, PA: Elsevier Ltd; 2016:159-162.
2. Craig LE, Julian ME, Ferracone JD. The diagnosis and prognosis of synovial tumors in dogs: 35 cases. *Vet Pathol*. 2002; 39(1):66-7.
3. Craig LE, Krimer PM, Cooley AJ. Canine synovial myxoma: 39 cases. *Vet Pathol*. 2010; 47(5):931-6.
4. Craig LE, Thompson KG. Tumors of joints. In: Meuten DJ ed. *Tumors in Domestic Animals*. 5th ed. Ames, IA: John Wiley and Sons Inc; 2017:337-350.
5. Izawa T, Tanaka M, Aoki M, Ohashi F, Yamate J, Kuwamura M. Incidental synovial myxoma with extensive intermuscular infiltration in a dog. *J Vet Med Sci*. 2012; 74(12):1631-3.

CASE II: JPC WSC-2 (JPC 4069828).

Signalment: Five-month-old Hereford-crossbred steer (*Bos taurus*).

History: Calves fed potatoes, 1 death in the herd. Calf showed neurological signs, focal seizures, blindness, head pressing. No response to thiamine or florfenicol.

Gross Pathology: The brain gyri were swollen and flattened. The rumen pH was 8, and the rumen contained two, small balls of plastic bags. The jejunum had several *Monezia expansa* cestodes. The costochondral junctions had a 7mm-thick, dense line of presumed cartilage core retention. Radiographs of thin sections have a dense white line.

Laboratory results: Blood lead concentration: 0.7 ppm (normal <0.3 ppm) Kidney lead concentration: 6.2ppm (Normal: 0.1-1.0 ppm) Hematocrit: 31%.

Histopathologic Description: A section of decalcified rib costochondral junction is examined. The zone of proliferating chondrocytes is longer than expected and proliferating chondrocytes can be seen in trabeculae far into the rib in retained, calcified cartilage. The invasion into chondrocytes is uneven, and while osteoblasts pile up in the hollow profiles of early-calcified chondrocytes, osteoclasts do not extend into these chondrocytes. The chambers of the initially invaded chondrocytes have erythrocytes, and a punctate, <2um basophilic "dusting" often fills these early chambers. The provisional calcified cartilage is retained far into the rib marrow space with only thin, apposed osteoid/bone. The provisional bone is thick and retained. Some osteoclasts are free in the marrow as opposed to being apposed to surfaces. Osteoclasts show more ani-socytosis with both size and shape variation and variable numbers of nuclei (osteoclastic dysplasia). Many dysplastic osteocytes have large, round and multiple inclusions. Bone marrow is otherwise hypocellular with serous degeneration of fat, and normal marrow constituents of the rib appear more distal from the costochondral junction than in a normal physis.

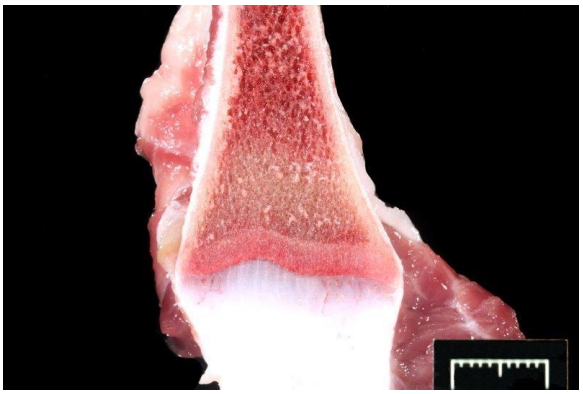

Rib, calf: The costochondral junctions had a 7mm-thick, dense line of presumed cartilage core retention (Photo courtesy of: Dept Vet Pathobiology, College Vet Med Biomed Sciences, Texas A&M University, http://vetmed.tamu.edu/vtpb)

Contributor's Morphologic Diagnosis: Rib, physis: chondrodystrophy with osteo-sclerosis, retained calcified cartilage**;** osteoclast dysplasia/hyperplasia.

Contributor's Comment: Costochondral line examination is part of a routine diagnostic necropsy examination. It demonstrates nutritional imbalances in any production mammal, or as in this case, mineralized cartilage retention usually due to osteoclast "problems" such as with BVDv persistently infected calves, canine distemper (Thompson 2007), and in our case, lead poisoning. Unfortunately, many people do not do it routinely.

The bone lesions of lead poisoning were well described in the early 1930's by several

Rib, calf: Radiographs of thin sections have a dense white line. (Photo courtesy of: Dept Vet Pathobiology, College Vet Med Biomed Sciences, Texas A&M University, http://vetmed.tamu.edu/vtpb)

authors studying poisoned children, and those descriptions remain valid. (Reviewed by Park 1933). The lead line in children will form once blood lead is 70-80 ug/dl. One month after treatment with chelating agents, the line separates from the zone of proliferating chondrocytes, and it will disappear in 4 years (Sachs 1981). Later descriptions added electron microscopic findings indicating that osteoclasts often lost their ruffled border and were less intimate with the surfaces (Eisenstein 1975). Nuclear and cytoplasmic inclusions were seen with EM. The cytoplasmic inclusions increased in size in osteoclasts more distant from the physis (inclusions fused?). Ultimately, morphologists concluded there is an inability for chondroclasts/osteoclasts to remove metaphyseal calcified cartilage cores presumably because they cannot degrade (or excrete) it. "They are thus constipated."(Eisenstein 1975) Interestingly, lead binds to osteocalcin to make a more compact molecule, and lead can cause a 40% increase of hydroxyapatite mineral over that bound with calcium (Dowd 2008). Might such modifications lead to "indigestion"- to continue the ANALogy (JFE)? The increase in osteoclasts is a compensatory hyperplasia. Lead poisoning-induced, osteoclast intra-nuclear inclusions are visible with electron microscopy (Hsu 1973). These inclusions of lead and protein aggregates are best-known in proximal renal tubules (where they make up 90% of the lead in kidneys), but are also in osteoclasts and less frequently in hepatocytes and glia (Goyer 1970, Moore 1974). Experimental and spontaneous studies demonstrate they may appear and regress in intoxicated individuals (Hzu 1973, Hamir 1983, Goyer 1970). EM shows them more frequently, and they are seen occasionally in light microscopy using Ziehl-Neelsen acid-fast stain. We could not see them reliably with acid-fast or PAS staining. In experimental lead poisoning of dogs (Zook 1972), metaphyseal sclerosis with retention of cartilage trabeculae having "more mineralized cartilage" with increased numbers of large osteoclasts distal from the physis were seen.

Obviously, the lines are seen in young animals' forming bones. Lead intoxication is more common in calves and thus are seen during calving season. Cattle usually have exposure to old lead base paints, discarded lead batteries, solder, linoleum, mining, smelting, and crankcase oil (ingested or used on skin as an insect repellant!) in pens or pastures (Blakley 1984, Burren 2010). Sometimes, recycling materials are incriminated (Payne 2008). Cases where pastures are previous shooting ranges have produced lead intoxications (Payne 2013). The decreased use of leaded gasolines has reduced risk of lead poisoning (Burren 2010). Blood, liver and kidney are favored samples to measure lead. When examining

blood, many animals having measurable blood lead will not show signs (diarrhea, seizures, bruxism, blindness, hemorrhages). The half-life of lead in exposed cattle is 135 days, std deviation 125 days (Bischoff 2012, Voigt 2010). Our calf was ill and had laminar cortical necrosis. Unfortunately, a specific lead source in this case was not found, and a farm visit was not allowed. The potatoes mentioned in the history were never provided and are considered a red herring.

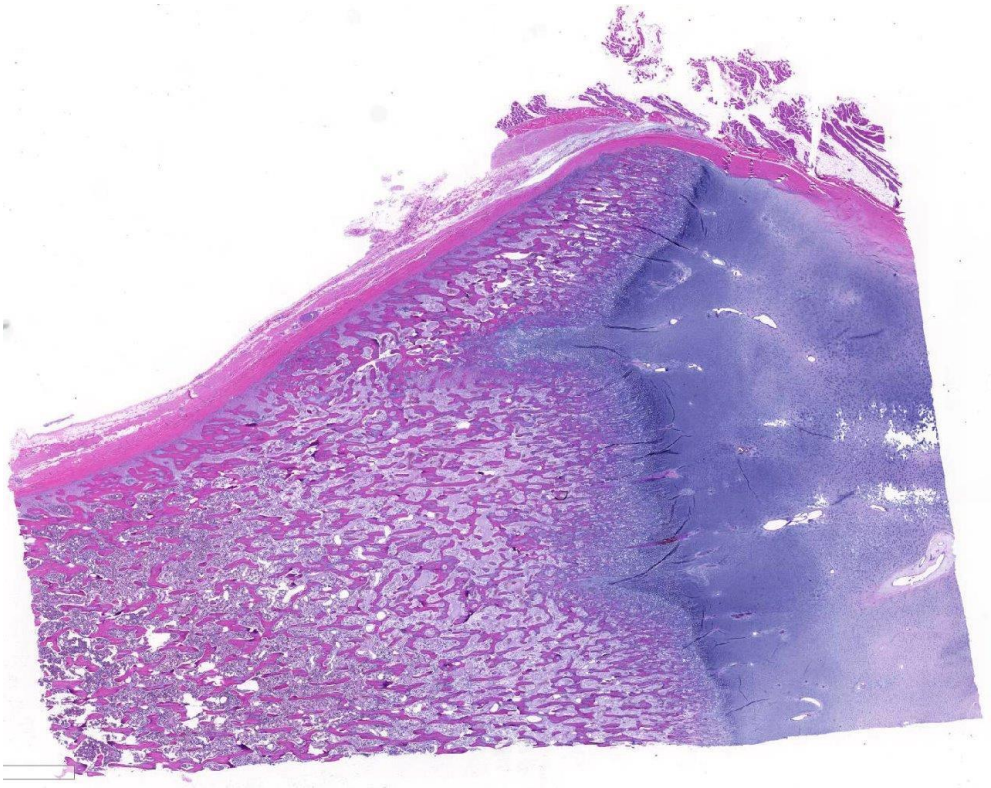

Rib, calf: Subgross magnification of the submitted tissue show a diffusely thickened epiphysis with two tongues of retained cartilage extending into the metaphysis. (HE, 5X)

JPC Diagnosis: Lone bone: Physeal dysplasia, with retention of cartilage cores, and focal necrosis, Hereford-crossbred steer, *Bos taurus*.

Conference Comment: We thank the contributor for his thorough and often satirical review of the skeletal lesions associated with lead toxicity in a young growing animal. The excellent quality gross image and radiographs provided by the contributor nicely demonstrate the thick band of sclerosis present in the metaphysis, known as the "lead line" mentioned above. Normally, growth of the bone at the metaphysis is the result of an orderly balance between osteoblastic deposition of bone and osteoclastic bone resorption at the zone of provisional calcification in the physeal zone of hypertrophy and primary spongiosa.[4,11] The majority of lead is stored within osseous tissues of the skeleton, and lead ions will preferentially deposit within the metaphysis and directly inhibit osteoclastic activity at this location.[16] As a result of this impairment of osteoclastic resorption of bone within the primary spongiosa, there is disruption of endochondral ossification and the formation of a growth retardation lattice.[4,11,16] This lattice is composed of elongated and vertically oriented trabecular bone with persistent cores of mineralized cartilage within the metaphysis. The sclerotic metaphysis is not radiopaque due to the lead itself; rather it is a result of calcium deposition and retention of mineralized cartilage trabeculae within the metaphysis.[4,11] As mentioned by the contributor, other diseases that cause growth retardation lattices include canine distemper virus (canine morbillivirus) and bovine

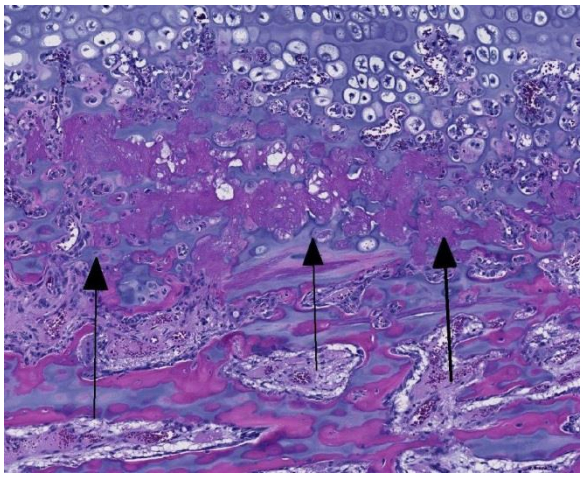

Rib, calf: Retained cartilage cores are lined by a necrotic coagulum (arrows). (HE, 88X)

pestivirus. Both viruses infect osteoclasts resulting in reduced bone resorption.[4,11]

This case generated spirited discussion among conference participants regarding whether the histologic lesions described in this case are consistent with lead intoxication. Conference participants described a diffusely thickened growth plate with multifocal tongues of cartilage cores extending into the metaphysis with a light blue to pink matrix and surrounded by a necrotic coagulum. Participants also noted few large vacuolated osteoclasts containing up to thirty nuclei within Howship's lacuna but were not able to identify intranuclear or intracytoplasmic inclusions noted by the contributor.

Prior to the conference, the moderator, Dr. Linden Craig, examined the long bones of several age-matched control calves without lead intoxication. The consensus opinion of the conference moderator and participants is that there is no significant difference between the amount of mineralized cartilage trabeculae in the calf from this case and an aged matched control animal. This represents a disconnect between the sclerotic metaphysis seen both grossly and radiographically in this case, and the histologic appearance which lacks the significant retention of mineralized cartilage trabeculae within the metaphysis when compared to the rib of age-matched control. Some participants posited that this may be an artifact of decalcification processing of this section. Without the aid of the gross, radiographic, and historical data, diagnosis of lead intoxication in this case is extremely difficult.

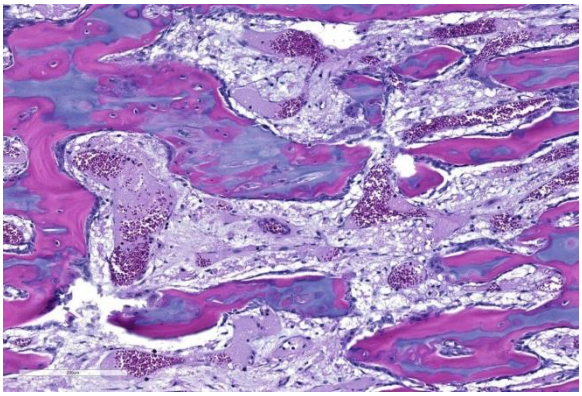

Rib, calf: Marrow spaces within the metaphysis are devoid of marrow elements. (HE, 152X)

Contributing Institution:
Department of Vet Pathobiology
College of Veterinary Medicine Biomed Sciences
Texas A&M University
http://vetmed.tamu.edu/vtpb

References:

1. Bischoff K, Thompson B, Erb HN, Higgins WP, Ebel JG, Hillebrandt JR. Declines in blood lead concentrations in clinically affected and unaffected cattle accidentally exposed to lead. *J Vet Dign Invest*. 2012; 24:182-7.
2. Blakley BR. A retrospective study of lead poisoning in cattle. *Vet Hum Toxicol*. 1984; 26: 505-7.

3. Burren BG, Reichmann KG, McKenzie RA. Reduced risk of acute poisoning in Australian cattle from used motor oils after introduction of lead-free petrol. *J Aust Vet Asso*. 2010; 88: 240-241.
4. Craig LE, Dittmer KE, ThompsonKG. Bones and joints. In: Maxie MG, ed. *Jubb, Kennedy and Palmer's Pathology of Domestic Animals*. Vol 1. 6th ed. Philadelphia, PA: Elsevier Ltd; 2016:16-87.
5. Dowd TL, Li L, Gundberg CM. The 1H NMR structure of bovine PB2-osteocalcin and implications for lead toxicity. *Biochim Biophys Acta*. 2008; 1784:1534-45.
6. Eisenstein R, Kawanoue S. The lead line in bon-A lesion apparently due to chondroclastic indigestion. *Am J Pathol*. 1975; 80: 309-16.
7. Goyer RA, May P, Cates M, Krigman MR. Lead and protein content of isolated intranuclear inclusion bodies from kidneys of lead-poisoned rats. Lab Invest. 1970; 22:245-251.
8. Hamir AN, Sullvan ND, Handson PD. Acid fast inclusions in tissues of dogs dosed with lead. J Comp Pathol. 1983; 93:307-17.
9. Hsu FS, Krook L, Shively JN, Duncan JR. Lead inclusion bodies in osteoclasts. *Science*. 1973; 181:447-8.
10. Moore JF, Goyer RA. Lead-induced inclusion bodies. Composition and probable role in lead metabolism. *Environ Health Perspec*. 1974; 7:121-7.
11. Olson EJ, Carlson CS. Bones, joints, tendons, and ligaments. McGavin MD,ed. *Pathologic basis of Veterinary Disease*. 6th ed. St. Louis, MO: Elsevier Mosby; 2017:964-965.
12. Park EA, Jackson D, Goodwin TC, Kajdi L. X-ray shadows in growing bones produced by lead; Their characteristics, cause, anatomical counterpart in the bone and differentiation. *J Pediatr*. 1933; 3: 265-300.
13. Payne JH, Holmes JP, Hogg RA, van der Burgt GM, Jewell NJ, Welchman G de B. Lead intoxication from clay pigeon shooting. *Vet Rec*. 2013; 173:552-4.
14. Payne J, Otter A, Cranwell M, Jones J, Wessells M, Whitaker K. Lead poisoning associated with recycled wood products. *Vet Rec*. 162: 191-2.
15. Sachs HK. The evolution of the radiographic lead line. *Radiol*. 1981; 139: 81-85.
16. Thompson K: Bones and joints. In: Maxie MG ed. *Jubb Kennedy and Palmer's Pathology of Domestic Animals*, 5th edition. Saunders Elsevier New York; 2007:53-54.
17. Voigt K, Benavides J, Rafferty A Howie F, Buxton D. Lead poisoning in calves with eosinophilic meningitis. *Vet Rec*. 2010; 167:791-2.
18. Zook BC. The pathologic anatomy of lead poisoning in dogs. Vet Pathol. 1972; 9, 310-327.

CASE III: 16N0558 (JPC 4084206).

Signalment: Nineteen-year-old quarter horse mare (*Equus ferus caballus*).

History: The horse presented to the teaching hospital for severe acute onset of right front limb lameness, from Middletown in Lake County, California. According to the owner,

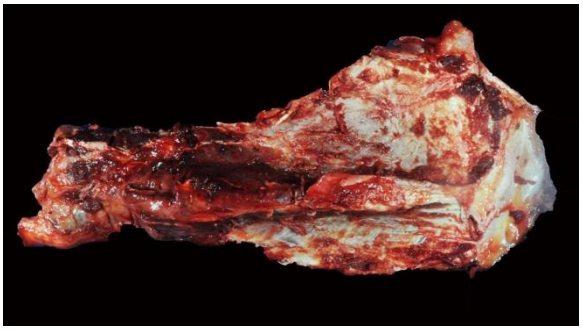

Scapula, horse: There is a transverse non-displaced fracture of the scapular neck and hemorrhage and edema within surrounding soft tissue (Photo courtesy of: University of California, Davis School of Veterinary Medicine, Veterinary Medical Teaching Hospital, Anatomic Pathology Department http://www.vetmed.ucdavis.edu/vmth/small_animal/anatomic_pathology/)

abnormal posturing began two weeks prior to presentation, and the horse was described as tucking its hind legs under itself. At that time, titers were negative for equine protozoal myeloencephalitis. Physical exam revealed toe dragging lameness of the right forelimb and asymmetric shoulder muscle atrophy, most pronounced on the right side. Radiographs of the proximal aspect of the right forelimb demonstrated a lytic bone lesion in the proximal scapula. In addition, multifocal heterogeneous mineral dense nodules were observed following the trachea from the thoracic inlet (cranial mediastinal lymph nodes), to the hilar region (tracheobronchial, caudal mediastinal lymph nodes). Ultrasound of the right scapula identified a severely irregular bone margin with mixed echogenicity, and soft tissue masses within the overlying skeletal muscle. A soft tissue sarcoma was suspected based on results from a fine needle aspirate of the masses.

Gross Pathology: Gross examination of the right scapula identified moderate hemorrhage and edema within the surrounding soft tissue as well as exuberant periosteal callus formation associated with a complete transverse, non-displaced fracture of the scapular neck. The skeletal muscle proximal to the fracture callus was diffusely atrophied, firm, pale, and intersected by bands of fibrosis. A second, more chronic complete fracture of the left supraglenoid tubercle was also identified. There were multifocal to coalescent regions of circumferential, porous cortical expansion of the ribs. Multiple, well-demarcated areas of bright red cortical discolouration were noted in the humeri. These lesions corresponded to regional osteolysis on clinical and post-mortem radiographs. The mineralized masses within the thorax were identified as enlarged, mineralized mediastinal and tracheobronchial lymph nodes

Laboratory results:

Biochemistry: (normal range)

Mild increase in creatinine kinase 348 IU/L (119-287)

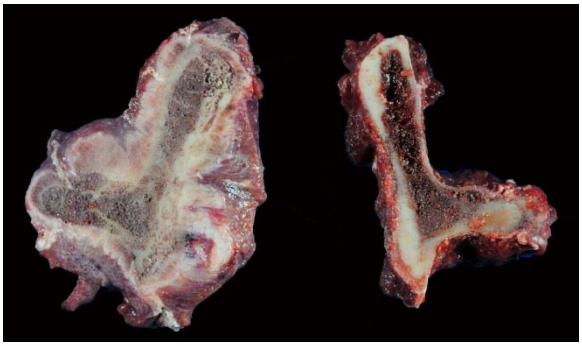

Scapula, horse: Sagittal section of the affected scapula (at left). (Photo courtesy of: University of California, Davis School of Veterinary Medicine, Veterinary Medical Teaching Hospital, Anatomic Pathology Department http://www.vetmed.ucdavis.edu/vmth/small_animal/anatomic_pathology/)

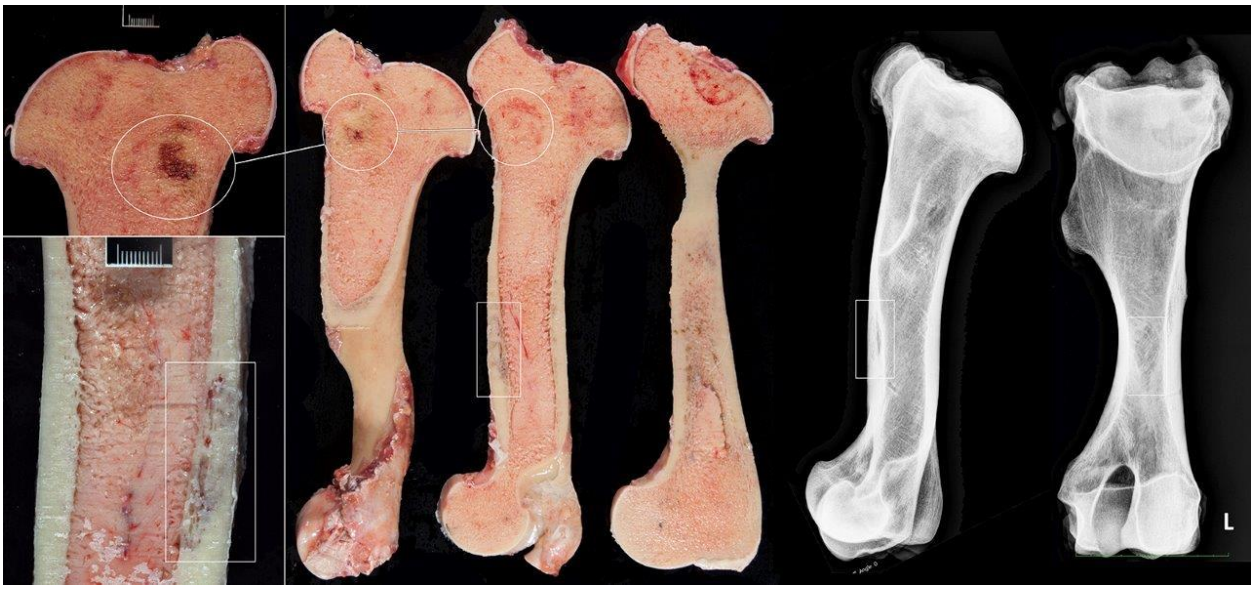

Scapula, horse: Multiple, well-demarcated areas of bright red cortical discoloration were noted in the humeri. (Photo courtesy of: University of California, Davis School of Veterinary Medicine, Veterinary Medical Teaching Hospital, Anatomic Pathology Department http://www.vetmed.ucdavis.edu/vmth/small_animal/anatomic_pathology/)

Histopathologic Description: Bone: The slide contains a single section of demineralized bone that lacks cortico-medullary distinction and consists of variably oriented and shaped, anastomosing osteochondral trabeculae. The section is embedded within and partially encased by a regionally necrotic and inflamed fibrovascular stroma. Dense fibrous and mildly congested tissue interdigitates with trabeculae at one section margin (presumed periosteal surface). Eighty percent of the bony trabeculae are composed of immature (woven) bone, and some contain cartilage. Lamellar bone is only preserved within larger trabeculae. Sharp edges, numerous, coalescing resorption bays (Howship's lacunae), and variation in trabecular shape and size is a result of resorption by large, hyperactive osteoclasts present in large numbers throughout the section. Osteoclasts contain up to 30 nuclei with often prominent eosinophilic nucleoli. Osteoclastic nuclei are occasionally arranged into circles resembling Langerhans giant cells. Osteoclasts are particularly abundant around the necrotic focus engulfing small shards of necrotic bone (presumed region of previous trauma) and some are noted within the surrounding stroma not adhered to the bone. Hyperactive osteoblasts accompany the osteoclasts and line most of the bone surfaces. A mosaic pattern of cement lines indicate ongoing dysregulated bone remodeling characterized by exuberant, seemingly random osteolysis and compensating osteoblastic activity. Inter-trabecular spaces are largely devoid of hematopoietic elements and filled by edematous, congested and mildly inflamed fibrous connective tissue. Inflammation consists of plasma cells, lymphocytes, and macrophages. Macrophages occasionally contain granular brown to golden cytoplasmic pigment (hemosiderin). Thin interlacing trabeculae of woven bone extend

There is extensive mineralization of the tracheobronchial lymph nodes. ((Photo courtesy of: University of California, Davis School of Veterinary Medicine, Veterinary Medical Teaching Hospital, Anatomic Pathology Department http://www.vetmed.ucdavis.edu/vmth/small_animal/anatomic_pathology/)

outwards from the presumed periosteal surface into the surrounding dense fibrous tissue (periosteal new bone formation vs callus).

Contributor's Morphologic Diagnosis: Bone, scapula: Severe, chronic, multifocal to coalescing osteolysis with atypical osteoclasts, aberrant bone remodeling, medullary fibrosis, and multifocal necrosis (consistent with silicate associated osteoporosis).

Contributor's Comment: Histologic examination of the tracheobronchial lymph nodes confirmed the presence of numerous fibrosing and mineralizing granulomas that contained moderate amounts of birefringent crystalline material. This finding, in conjunction with the osteoporotic skeletal lesions, and the geographic origin of the horse (from a location known to contain toxic soil silicate dioxide (cristobalite)) are consistent with a diagnosis of silicate associated osteoporosis (SAO). Without additional clinical information and knowledge of the bone sample skeletal site, differential diagnoses for this histological slide should broadly include a metabolic bone disease. For example, hyperactive osteoclasts and poor construction of new bone may be seen with fibrous osteodystrophy as a result of Ca++/P imbalance, variable nutritional deficiencies, vitamin D deficiency, and endocrinopathies.[4]

Pulmonary silicosis has been previously reported in both humans and horses, however, the associated osteoporotic syndrome appears unique to equids.[1] The underlying pathogenesis for this condition has yet to be elucidated.

Affected horses present with vague acute or chronic signs of lameness, often accompanied by weight loss, and variably by clinically evident pulmonary disease. Horses may appear to have bowing of one or both scapulae and accentuated lordosis. Acute lameness may be observed secondary to pathologic fractures often with ineffective attempts at repair as observed in this case. If

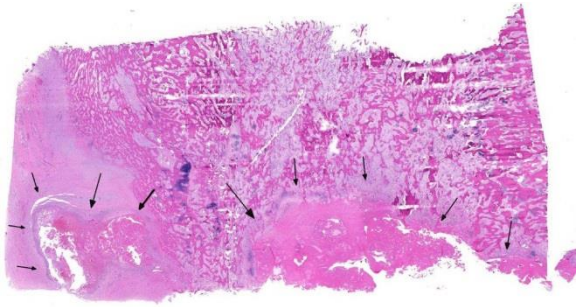

Scapula, horse: Subgross view of the submitted section of scapula. There is no evidence of cortical bone, and the section is composed of haphazardly arranged trabeculae of woven and lamellar bone, as well as extensive areas of necrotic bone. (HE, 6X)

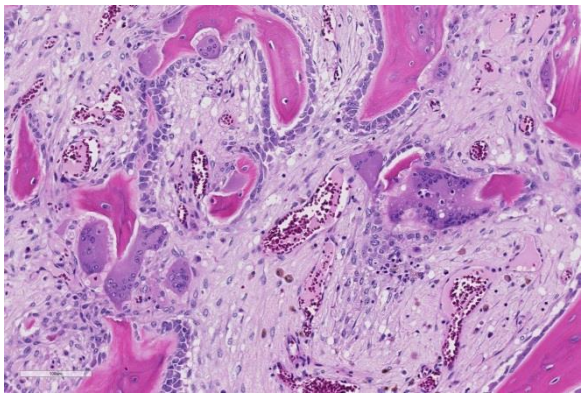

Scapula, horse: Osteoclasts are numerous, and in some cases, extremely large. (HE, 172X)

clinically silent, chronic fibrosing granulomas within the lung-draining lymph nodes and variably within the lungs are usually identified postmortem. Thoracic radiographs may detect an interstitial pattern of consolidated pulmonary nodules, but will often miss mineralized, lung-associated lymph nodes. Histologic examination of the granulomas reveals the typical pattern of central necrosis, marked fibrosis and mineralization surrounded by epithelioid macrophages and occasional giant cells. Small, angular, birefringent, intra- and extra-cellular crystals may be revealed under polarized light. The exorbitant reaction associated with such crystals is unique to the toxicity of cristobalite as compared to relatively innocuous accumulations associated with common anthracosilicotic nodules. Electron diffraction crystallography has been used to confirm the physical characteristics of crystals as cristobalite, (technique available in geology laboratories that analyze soil or stones).

Clinical and postmortem radiographs of the axilla and proximal appendicular skeleton are non-specific but may reveal poorly demarcated areas of osteoporosis and confirm bone deformity. Finding cervical facet joint osteoarthrosis is common in advanced cases of SAO. The radiographic appearance of bone lesions is variable but can be mistaken for neoplasia driven osteolysis as observed in this case.

Currently, the most sensitivity pre-mortem diagnostic test for this condition is bone nuclear scintigraphy.[4] The search for sensitive and specific clinical markers to detect early onset of the disease is ongoing.

Histologic examination of the affected bone reveals dysregulated resorption by morphologically atypical giant hyperactive osteoclasts.[1] Typical of SAO, the osteoclasts indiscriminately resorb pre-existing cortical and trabecular bone as well as newly formed woven bone. A mosaic pattern of cement lines is commonly observed in SAO bones; this microscopic feature is shared by human Paget disease of bone.[6] Multifocal areas of bony lysis, aberrantly increased regions of bone remodeling, pathologic fractures and aberrant giant osteoclasts are other similarities observed between these two disorders.[1] However, polyostotic Paget disease is restricted to specific age groups (elderly humans) and exhibits cessation of osteoclast activity over time. In contrast, SAO is observed in horses of all ages and shows progression of disease with time.[1,5] In addition, the skeletal distribution of SAO does not correspond with that observed in Paget disease.[1] The lesions of SAO have also been compared to fibrous osteodystrophy, however, skull lesions are uncommon in horses with SAO and only a

subset of affected horses exhibit elevations in parathyroid hormone.[1]

Unusual features of this case include the effacement of hematopoietic tissue within the medullary cavity and the identification of gross and radiographic lesions with the humeri.

JPC Diagnosis: Bone: Abnormal bone remodeling with myelofibrosis, proliferation of numerous large atypical osteoclasts, and focally extensive necrosis, quarter horse, *Equus ferus caballus*.

Conference Comment: This challenging case confounded even the most senior and experienced conference participants. Due to the lack of a recognizable corticomedullary junction or physiologic tissue border combined with severe distortion of the tissue by the disease process, attendees were unable to determine the type of bone this tissue section represented. Participants were impressed by the extensive and aberrant bone remodeling and resorption by atypically large and randomly located osteoclasts with vacuolated foamy cytoplasm and up to 30 supernumerary nuclei. These nuclei are sometimes arranged in circles resembling Langerhans giant cells in this section of bone. The constellation of lesions in this case combined with the historical data raise the index of suspicion for equine bone fragility syndrome (BFS), also known as silicate associated osteoporosis (SAO), although, as mentioned by the contributor, other metabolic bone diseases should also be considered as differential diagnoses.[1,2]

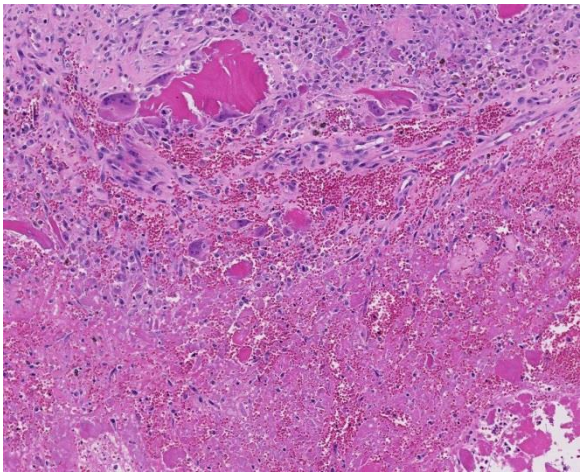

Scapula, horse: In the area of the fracture, there is abundant necrotic bone, granular debris, and hemorrhage, surrounded by a layer of granulation tissue. Bone fragments are being resorbed by multinucleated giant cell macrophages. (HE, 84X)

The pathogenesis and cause of bone fragility syndrome in horses is unknown. The vast majority of affected horses present concurrently with pulmonary silicosis and there is likely a causal relationship between the two conditions. As mentioned by the contributor, pulmonary silicosis, defined as silicate pneumoconiosis with accompanying pulmonary fibrosis, occurs secondary to inhalation of cytotoxic silica dioxide (SiO2) crystal polymorphs, including quartz, cristobalite, and tridymite.[1,2,3] Pulmonary silicosis with concurrent bone fragility syndrome has been reported with increased frequency in horses from areas with high levels of soil cristobalite, such as Monterey, Napa, and Sonoma regions of California; however, affected horses have also been seen in Oregon, Texas, Virginia, Illinois, and Kentucky.[1,2,3] The cytotoxic crystals associated with pulmonary silicosis are found worldwide, perhaps suggesting that this disease may be more widespread.[1,2] Readers are encouraged to review 2015

Wednesday Slide Conference #3 Case 4 for an excellent review of a suspected case of pulmonary silicosis in a horse from Monterey, California.

It is thought that the inhaled silicate stimulates the massive release of proinflammatory cytokines, IL-1, IL-6, and TNF-alpha, which stimulate inflammation and osteoclastogenesis via increased production of the RANKL and decrease in expression of the decoy receptor, osteo-protegerin.[1] Other proposed mechanisms of pathogenesis include hyperparathyroidism or an equine variant of Paget disease of bone in humans.[1,2]

Horses with bone fragility usually present with chronic lameness and skeletal deformities such as lateral bowing of the scapulae, lateral bowing of the rib cage, lordosis, and decreased range of motion in the cervical vertebrae.[1,2] Bones of both the axial and proximal portions of the appendicular skeleton, such as the scapula, in this case, are typically affected. Radio-graphically, there is severe osteopenia with multiple bony lucencies and exostoses at the articular facets as well as thickening of the rib consistent with extensive bone remodeling.[1,2] As a result of the severe osteoporosis associated with this disease entity, most animals die from a catastrophic pathologic fracture.[1,2] Conference participants noted that the large focally extensive area of necrosis in this tissue section may be the site of a pathologic fracture of the scapula.

Contributing Institution:

University of California, Davis
School of Veterinary Medicine
Veterinary Medical Teaching Hospital
Anatomic Pathology Department
http://www.vetmed.ucdavis.edu/vmth/small_animal/anatomic_pathology/

References:

1. Arens AM, Barr B, Puchalski SM, et al. Osteoporosis associated with pulmonary silicosis in an equine bone fragility syndrome. *Vet Pathol*. 2011; 48(3):593-615.
2. Arens AM, Puchalski SM, Whitcomb MB, et al. Comparison of the use of scapular ultrasonography, physical examination, and measurement of serum biomarkers of bone turnover versus scintigraphy for detection of bone fragility syndrome in horses. *J Am Vet Med Assoc*. 2013; 242(1):76-85.
3. Berry CF, OBrien TR, Madigan J, Hager DA. Thoracic radiographic features of silicosis in 19 horses. *J Vet Intern Med*. 1991; 5:248-256
4. Carlson CS, Weisbrode SE. Bones, joints, tendons, and ligaments. In: McGavin MD, Zachary JF, eds. *Pathologic Basis of Veterinary Disease*. 5th ed. St. Louis, MO, PA: Mosby Elsevier; 2012.
5. Symons JE, Entwistle RC, Arens AM, et al. Mechanical and morphological properties of trabecular bone samples obtained from third metacarpal bones of cadavers of horses with a bone fragility syndrome and horses unaffected by that syndrome. *Aust Vet J*. 2012; 73(11):1742-1751.
6. Seitz S, Priemel M, Zustin J, et al. Paget's disease of bone: histologic analysis of 754 patients. *J Bone Miner Res*. 2009; 24:62-69.

CASE IV: P3554.15 (JPC 4084557).

Signalment: 11-year-old castrated male domestic cat (*Felis catus*).

History: This cat presented with a history of chronic vomiting and weight loss. A firm and fixed intra-abdominal mass was palpated during physical examination. The mass consisted of a group of enlarged mesenteric lymph nodes and adjacent thickened intestinal wall at the ileocecocolic junction. The lymph nodes and a 20 cm-long intestinal segment were resected (limit between the normal and pathologic intestine not clear).

Gross Pathology: The mesenteric lymph nodes were moderately enlarged, irregular, white to pink, firm and gritty on cut section. The intestinal wall at the ileocecocolic junction was diffusely and severely thickened and focally expanded by a firm, multilobulated mass, 7 cm in diameter that partially occluded the lumen.

Laboratory results: N/A

Histopathologic Description: Mesenteric lymph node: The parenchyma is extensively effaced and replaced by thick branching and anastomosing, weakly cellular trabeculae of dense collagen separated by plump spindle-shaped cells (sclerosing fibroplasia) admixed with inflammatory cells, mainly eosinophils with fewer plasma cells, lymphocytes, mast cells and neutrophils. At the periphery of the sclerosing fibroplasia, spindle cells with fine branching collagen fibers dissect and efface the lymphoid tissue accompanied by a dense infiltrate of eosinophils. The remaining lymphoid tissue shows moderate follicular lymphoid hyperplasia. The branching collagen trabeculae were strongly positive for picrosirius red. Toluidine blue staining was performed to eliminate the possibility of a mast cell tumor.

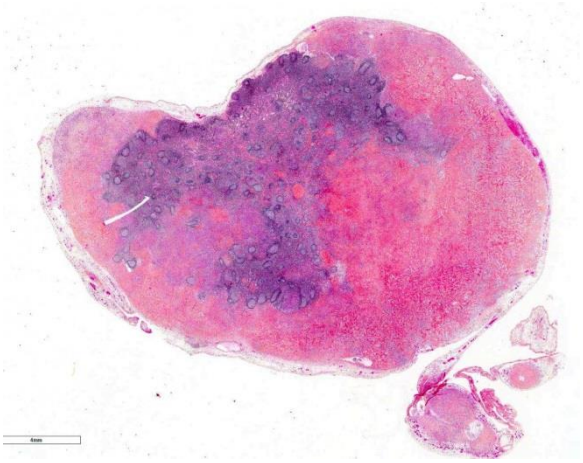

Mesenteric lymph node, cat. The periphery of the node is effaced by anastomosing trabeculae of fibrous connective tissue. The node is reactive as evidenced by prominent follicles. (HE, 6X)

Intestinal wall/mass (not submitted): Lesions similar to the mesenteric lymph nodes diffusely efface and replace the ileocecocolic submucosa and tunica muscularis, focally creating a mass effect. The mucosa has markedly increased numbers of eosinophils (lamina propria), and is multifocally and extensively ulcerated with granulation tissue. The lumen contains fibrinonecrotic debris admixed with numerous bacteria.

Contributor's Morphologic Diagnosis: Mesenteric lymph node: Eosinophilic lymphadenitis, marked, focally extensive, with sclerosing fibroplasia. Lesions are typical of feline gastrointestinal eosinophilic sclerosing fibroplasia (FGESF).

Contributor's Comment: Feline gastro-intestinal eosinophilic sclerosing fibroplasia (FGESF) is a recently described feline inflammatory condition affecting the gastrointestinal tract and associated lymph nodes.[1] FGESF is primarily a condition of

middle-aged cats although feline of almost any age can be affected. Male cats and the Ragdoll breed were overrepresented in a review of 13 cases.[5] Affected cats are usually presented with digestive signs, including vomiting, diarrhea, weight loss and inappetence. An abdominal mass is frequently detected, either by palpation or imaging and sometimes associated with regional lymphadenopathy. The mass most commonly occurs at the pyloroduodenal or ileocecocolic junction but can be found elsewhere along the intestines.[1,5] Bloodwork abnormalities that can be associated with this condition include hyperproteinemia associated with hyperglobulinemia, hypoalbuminemia, peripheral eosinophilia and mild neutrophilia.[5,8]

Histologically, FGESF lesions exhibit a characteristic pattern made of a network of coarse collagen trabeculae admixed with a large spindle cell population identified as myofibroblasts[1] mixed with inflammatory cells including numerous eosinophils.[1,5,7,8] The fibroplasia and inflammatory response extensively infiltrate the intestinal wall and, sometimes, regional lymph nodes. The intestinal mucosa is frequently ulcerated. Grossly and histologically, FGESF may resemble neoplasia, particularly, fibrosarcoma and extra-skeletal osteosarcoma; thus, FGESF must be included in the differential diagnosis of cats presented for abdominal mass and/or mesenteric lymphadenopathy.

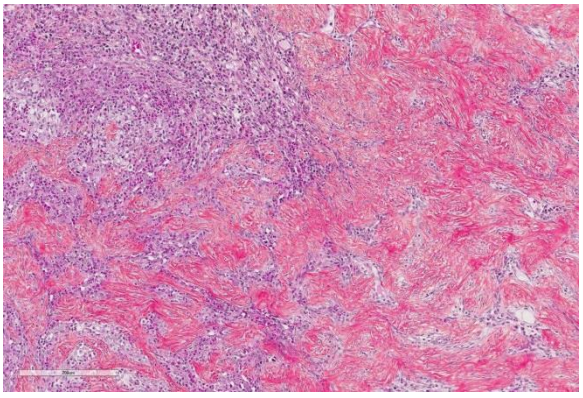

Mesenteric lymph node, cat. Higher magnification of the affected node, showing anastomosing collagenous trabeculae separated by a cellular infiltrate. (HE, 144X)

The etiopathogenesis of this condition is still not completely understood. The presence of bacteria, including gram-positive cocci as well as gram-positive and gram-negative rods have been associated with lesions in several studies,[1,5,8] but it is still unclear how bacteria contribute to the development and/or perpetuation of the condition. The location of lesions in close proximity or communicating with the normal bacterial flora makes it complicated to establish an association. In one study, IHC was performed and was negative for both FHV-1 and FCoV/FIP viral antigens.[5] It was also hypothesized that affected cats could suffer from immunologic dysregulation triggered by one or few factors, including parasitism, food allergy, dysbiosis or certain forms of IBD but again, no clear associations have been made. Nevertheless, eosinophilic inflammation seems to be a critical feature of this condition and is consistently predominant. Eosinophils produce a variety of mediators, including major basic protein (MBP), TGF-β, Il-1b, IL-6, that lead to tissue destruction and fibrosis.[1,5,7,8] A perpetuating inflammatory and fibrotic process is thought to be responsible for the proliferative nature of the pathology that gives rise to an intra-abdominal mass. Prognosis varies from good to guarded since infiltration is sometimes extensive and not surgically resectable (if located at the pyloroduodenal junction) but survival times can be good with a combination of appropriate surgical and medical treatments.[1,5,8]

JPC Diagnosis: Lymph node: Lymphadenitis, eosinophilic, diffuse, moderate with

marked anastomosing fibroplasia and moderate follicular and paracortical hyperplasia, domestic cat, *Felis catus*.

Conference Comment: Despite moderate slide variability, conference participants agree that this case is an excellent example of the characteristic microscopic features associated with feline gastrointestinal eosinophilic sclerosing fibroplasia (FGESF), which often includes effacement of mesenteric lymph nodes by haphazard branching and anastomosing trabeculae of dense collagen admixed with spindle cells and numerous eosinophils. These firm nodular lesions are typically identified at the pyloric sphincter or ileocecocolic junction in domestic cats, but can also be present in the duodenum, jejunum, colon, and mesenteric lymph nodes, as in this case.[1,3,5] As mentioned by the contributor, the prognosis following surgical removal depends on the location of the nodule and the surgeon's ability to completely excise the mass without causing functional impairment of the gastrointestinal (GI) tract. As a result, lesions in the distal intestinal tract (ileocecocolic junction and colon) are associated with a better surgical prognosis than lesions encompassing the pyloric sphincter.[1,2,8]

Prior to the initial description and publication of this unique lesion in the feline GI tract by Craig et al, the characteristic trabeculae of dense collagen were often misinterpreted as osteoid, leading to an erroneous diagnosis of extra-skeletal osteosarcoma.[1] Additionally, the marked eosinophilic component admixed with scattered, well-differentiated, perivascular mast cells resulted in the interpretation of some of these lesions as feline sclerosing mast cell tumors.[4] In this case, histochemical staining with Masson's trichrome produced intense blue staining of the anastomosing

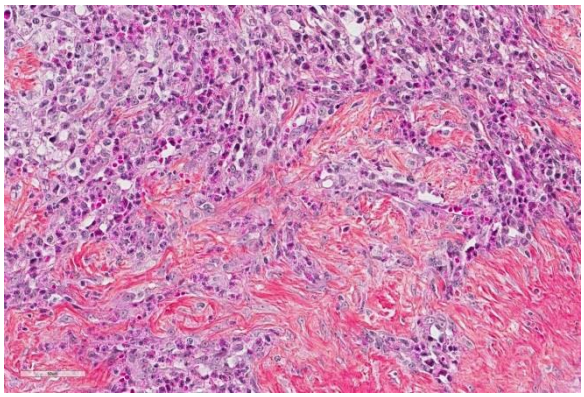

Mesenteric lymph node, cat. Higher magnification of the periphery of the mass, showing a dense, eosinophil rich inflammatory infiltrate enmeshed in fine fibrils of collagen. (HE, 400X)

trabeculae, confirming the presence of collagen.

Although the etiology and pathogenesis of this lesion is unknown, the conference moderator (Dr. Craig, referenced above) posits that it is likely an inflammatory process rather than neoplastic, similar to other feline eosinophilic inflammatory lesions, such as feline indolent ulcer, eosinophilic plaque, eosinophilic granuloma, and hypereosinophilic syndrome.[1,3] As mentioned by the contributor, the majority of previously reported cases are associated with bacterial infection, demonstrated by both gram-positive and gram-negative rods and cocci embedded within the sclerotic collagen;[1] however, there have been reports of FGESF associated with fungal infection, *Toxoplasma gondii* [1] and the alimentary nematode parasite (*Cylcoospirura* spp.) in a free-ranging puma. Additionally, there have also been reports of similar lesions present in the subcutis and abdomen of cats in Japan caused by methicillin-resistant *Staphylococcus* spp.[6]

Interestingly, in nearly half of reported cases by Craig, et al, no infectious etiology was detected.[1] In this case, a battery of histochemical stains run by the Joint

Pathology Center prior to the conference failed to reveal any infectious agents within dense bands of collagen. In cats that develop eosinophilic granulomatous disease, there may be an inherited genetic mutation leading to eosinophil dysregulation and inappropriate eosinophilic response to a variety of inflammatory stimuli.[1,3,7] This may contribute to the pathogenesis of this disease in certain predisposed individuals with or without evidence of an infectious agent.[1]

Contributing Institution:
Faculty of Veterinary Medicine
Université de Montréal
http://www.medvet.umontreal.ca/index.html

References:

1. Craig L, Hardam E, Hertzke D, et al. Feline gastrointestinal eosinophilic sclerosing fibroplasia. *Vet Pathol.* 2009; 46: 63–70.
2. Eckstrand CD, Barr BC, et al. Nematode-associated intramural alimentary nodules in pumas are histologically similar to gastro-intestinal eosinophilic sclerosing fibroplasia in domestic cats. *J Comp Pathol*. 2013; 148(4):405-409.
3. Grau-Roma L, Galindo-Cardiel I, et al. A case of feline gastro-intestinal eosinophilic sclerosing fibroplasia associated with phycomycetes. *J Comp Pathol*. 2014; 141:318-321.
4. Halsey CHC, Powers BE, Kamstock DA. Feline intestinal sclerosing mast cell tumour: 50 cases (1997-2008). *Vet Comp Oncol.* 2010; 8:72-79.
5. Linton M, Nimmo J S, Norris J M, et al. Feline gastrointestinal eosinophilic sclerosing fibroplasia: 13 cases and review of an emerging clinical entity. *J Feline Med Surg*. 2015; 17:392-404.
6. Ozaki K, Yamagami T, Nomura K, Haritani M, Tsutsumi Y, Narama I. Abscess-forming inflammatory granulation tissue with gram-positive cocci and prominent eosinophil infiltration in cats: Possible infection of methicillin-resistant *Staphylococcus*. *Vet Pathol*. 2003; 40:283–287.
7. Suzuki M, Onchi M and Ozaki M. A case of feline gastro-intestinal eosinophilic sclerosing fibroplasia. *J Toxicol Pathol*. 2013; 26:51-53.
8. Weissman A, Penninck D, Webster C, et al. Ultrasonographic and clinico-pathological features of feline gastrointestinal eosinophilic sclerosing fibroplasia in four cats. *J Feline Med Surg*. 2013; 15:148-154.